UNIVERSITI MALAYSIA PERLIS
International Journal of Nanoelectronics and Materials
IJNeaM
ISSN 1985-5761 | E-ISSN 2232-1535

Simulation and analysis of solar cells based on InN/p-Si: influence on thickness, doping concentration, and temperature dependence

Nur Syahirah Khairuddin[a], Mohd Zaki Mohd Yusoff[a,b*], Hanim Hussin[c], and Rosalio G. Artes Jr.[d]

[a]*School of Physics and Material Studies, Faculty of Applied Sciences, Universiti Teknologi MARA, 40450 Shah Alam, Malaysia*
[b]*NANO-SciTech Lab (NST), Centre for Functional Materials and Nanotechnology (CFMN), Institute of Sciences (IOS), Universiti Teknologi MARA, 40450 Shah Alam, Malaysia*
[c]*School of Electrical Engineering, College of Engineering, Universiti Teknologi MARA, 40450 Shah Alam, Selangor, Malaysia*
[d]*Mindanao State University Tawi-Tawi College of Technology and Oceanography, Philippines*
∗Corresponding author. Tel.: +603-55444560; fax: +603-55434562; e-mail: zaki7231@uitm.edu.my

Received 4 October 2023, Revised 28 February 2024, Accepted 12 March 2024

ABSTRACT

The current research project intends to enhance solar cells' power and conversion efficiency based on InN/p-Si utilizing the PC1D simulator. A broad direct bandgap of Indium nitride (0.65 eV) makes it suitable for various applications. The InN-based solar cells show an excellent candidate for generating a higher efficiency device, incorporating well-established silicon substrate technology. The open-source PC1D is well-known software for simulating future solar devices without the need to fabricate real devices. The simulated area was adjusted to 10 cm^2. The Si substrate and InN layer thicknesses were designed to be 350 μm and 1×10^{-3} μm, respectively. The n- and p-regions have doping concentrations of 1×10^{21} cm^{-3} and 1×10^{17} cm^{-3}, respectively. This work analyses the influence of geometrical and technological aspects such as both n-p regions thickness, doping concentrations, and temperature dependency to enhance the conversion efficiency of these structures under the AM1.5G solar spectrum with intensity 0.1 W/cm^2. It has been demonstrated that the growth of high-quality InN layers and p-type doping persists to be problematic. It appears challenging to find the most suitable material substrate for InN solar. To produce compatible solar cells with simple structures and cost-effective, however, extremely thin layers of n-layer material are required due to the high absorption coefficient of type III-nitrides. The results illustrate that by adjusting the optimized parameter at room temperature to the lowest temperature (200 K), the solar efficiency may increase up from 19.18% to 27.67%.

Keywords: *InN, Silicon, III-Nitrides, temperature dependence, solar cells, PC1D, efficiency*

1. INTRODUCTION

Researchers are getting more interested in type III-nitride semiconductors, such as gallium nitride (GaN), aluminium nitride (AIN), and indium nitride (InN), which have gaps of 3.4 eV, 6.2 eV, and 0.65 eV, respectively. III-nitrides semiconductors have been used widely in optoelectronics because of their reliability, high thermal conductivity, high melting temperature, and direct forbidden bandgap [1]. Wide direct band gap alloys are important materials in photovoltaic applications because they may be customized to fit the solar spectrum. They make excellent candidates for high-efficiency solar cells for challenging conditions or space applications due to their inherent characteristics, such as a high absorption coefficient, high carrier mobility, high drift velocity, excellent saturation velocities, high thermal stability and conductivity, and high radiation resistance [2]. In addition to their ability to enable the creation of third-generation solar cell types including intermediate band solar cells that are completely based on nitride alloys and multi-junction solar cells with high efficiency, these materials are incredibly helpful for photovoltaic applications. For multijunction solar cells, one of the junctions needs to be built of a material with a gap bigger than 2.4 eV in order to produce a terrestrial photovoltaic efficiency of above 50% [3]. Fascinating photovoltaic characteristics of III-Nitrides include low effective densities of charge carriers, great radiation tolerance, and extreme absorption coefficients [4]. The capacity of III-V nitride technology to generate high-quality optoelectronic devices and develop crystal structures has confirmed its potential for high-efficiency systems of solar cells [5]. In solar photovoltaic technology, silicon is the primary material. One of the main disadvantages of photovoltaic applications is the narrow and indirect band gap of silicon devices, which lowers the quantum efficiency of solar cells. Researchers were encouraged to investigate novel photovoltaic elements and structures using silicon cells, and one of their intentions was to produce solar photovoltaic cells based on III-nitrides elements [6].

Compared to gallium nitride (GaN) and aluminium gallium nitride (AlGaN) alloys, indium nitride (InN) solar cells can attain greater efficiencies; nevertheless, the greatest cell efficiency region is matched by indium gallium nitride (InGaN) alloys with intermediate energy gaps between InN and GaN materials [7]. The energy levels of electrons and holes fall as the electric field expands. The intermediate levels of electrons and holes are pushed out of their optimum positions by an increasing electric field, which

results in a decrease in photon absorption. As a result, the photo-generated current density J_{sc} falls. Consequently, efficiency declines when the electric field is increased [8]. The experimental method has been restricted by the high indium concentration observed in thick layers of InGaN. A major valence band offset is brought about by the indium's ability to accumulate in the active, affecting the cells' efficiency. In essence, the indium content is selected based on the band offset between GaN and InN [9]. In contrast, Si substrates are more expensive, larger, and more thermally and electrically conductive. After implementing silicon as a substrate in InGaN-based solar cells, the efficiency of power conversion and cost-effectiveness of the solar device are improved [10].

In the first-generation solar cell market, silicon exceeds all other materials due to its cost-effective cost and excellent interface quality. Additionally, silicon is widely available and has a developed technological background [11]. Nevertheless, It appears that there is little potential for improved performance or lower costs because the efficiency of silicon solar cells is approaching saturation [12]. This difference in efficiency is caused by the fact that only photons with energy greater than the energy gap are permitted to be absorbed in a typical photovoltaic system, such as a silicon-based p-n junction. However, a large part of the solar spectrum was left unexplored, and the photons that were not absorbed caused the device to heat up and lose some of its power efficiency [13]. Since InN has a lower dissociation temperature than AIN and GaN (500°C under vacuum), which reduces the ideal growth temperature for InN, producing high-quality InN has proven challenging [14]. Based on Imene's calculation of the energy gap of absorber material, the efficiency limit of single junction solar cells is predicted to be no higher than 31% under conditions of one-sun illumination and 300°K. [15]. For instance, it continues to be challenging to generate high-quality InN films and p-type doping [16]. Due to its low dissociation temperature (about 630°C), lack of substrates that match its lattice, high equilibrium nitrogen vapour pressure, and difficulty in preparing in stoichiometric form, InN is known to have the most difficult synthesis of any III-nitride molecule [17]. Additionally, high growth temperatures have the tendency to cause the metallic indium to separate from the crystal [18].

A PC1D simulation tool, which complements the experimental findings, is used to simulate photovoltaic solar cells. The PC1D simulation program is a commercially accessible tool that is frequently used for modeling solar cells [19]. The PC1D simulation software produces trustworthy and convincing results for the study of solar cells. Results using this tool are consistent with those from the experimental schemes. PC1D analysis of the degradation of a multi-junction solar cell under proton illumination and estimates of I_{sc} and V_{oc} obtained from simulations showed agreement with the experimental results with a 5% accuracy [20]. To determine the significant factors such as emission doping magnitude, wafer width, front and rear recombination, and bulk doping magnitude and their influence on solar cell performance, PC1D simulations were carried out on a variety of solar cell structures [21]. In order to determine the corresponding values of resistivity and diffusivity for the base layer's provided p- and n-regions and the emitter layer's mobility, PC1D first takes doping values for the base layer. Additionally, PC1D provides the option of enhancing the cell's performance by adding additional layers [22]. According to the PC1D simulation cells' performance parameters, there is an efficiency gain of between 22.1 % and 23.3 % [23].

The solar cell efficiency is mostly determined by the generation of photocurrent, which is greatly improved by the front layer thickness. The circuit current (I_{sc}), output circuit voltage (V_{oc}), current density (J_{sc}), fill factor, efficiency, and overall performance of the single junction-based InGaN solar cell are all influenced by the layer of absorber or thickness of the sensitizer [24]. The continuous adaptability of the direct bandgap of III-nitride semiconductors within the solar spectrum from the ultraviolet to the near-infrared makes them intriguing candidates for new electron-selective connections to p-region silicon heterojunction solar cells [25]. The appropriate value of minority carrier concentration is required to improve solar cell performance since surface recombination velocity is dependent on minority carriers and can affect solar cell conversion efficiency. As a result, temperature variations affect a variety of solar cell attributes, such as open-circuit voltage, short-circuit current density, fill factor, and efficiency [26]. Researchers suggested growing InN at low temperatures in order to prevent InN from thermally decomposing [27]. The efficiency of active nitrogen (N) atoms and a decrease in the kinetic energy of the reactants in the formation of InN bonds are both caused by the low growth temperature [28]. The short-circuit current density, J_{sc}, however, exhibits the inverse relationship with the band gap, rising with it when the band gap decreases because of an increase in the absorption coefficient and the corresponding rise in generation rate [29]. It should be noted that when the temperature rises, the band gap narrows, causing the short circuit to expand and the open circuit voltage to decrease [30]. The conversion efficiency decreases as the temperature rises because the photo-generated carriers are more likely to undergo recombination at higher temperatures [31].

The objective of these observations is to precisely determine the physical influence such as thickness regions and doping concentration of both p- and n- n-region material, hence figuring out the cause of the defects that may contribute to the performance of the solar cells. In addition to that, InN is a promising material for low-cost solar cells with high efficiency. The optimal manufacturing of InN and Si with band gap energies of 1.9 eV and 1.1 eV yields a conversion efficiency of more than 30% [32]. Because of its high drift velocity at room temperature, InN has proven to be the optimum material for high manufacturing efficiency solar cells and emitters with outstanding efficiency [33]. Despite the enormous progress, the second goal is to examine the optimized parameter of homojunction InN/p-Si solar cells with various operational temperatures and study the impact of high temperatures on the performance and conversion efficiency of solar cells.

2. METHODOLOGY

As a vital step towards comprehending the behaviour of the solar cell, the goal of this research is to analyse the effects of thickness and doping concentration on InN and Si regions in a solar cell. In order to determine and develop solar cell performance, the InN/p-Si photovoltaic solar cell was analysed using an analytical solar cell model at temperatures ranging from 200 – 400 K. Figure 1 depicts the conceptual device topology of the InN/p-Si single-junction solar cell under investigation. The base layer of the solar cell was made of Si, and the emitter layer was constructed of InN. In this study, the PC1D simulator program was chosen as the simulation tool due to its benefits, simplicity, and user-friendly interface. The PC1D simulator accepts doping values, which can be either n- or p-, and then calculates the corresponding resistivity and diffusivity values depending on the mobility and doping. Researchers state that the PC1D simulation method tends to achieve optimal performance with 70% target data compared to the experimental (30%) with satisfying results, where it led to additional performance gain, faster convergence, costly effectiveness and more robustness [34]. Researchers experimentally reported, that with high indium composition (x = 1.0), they managed to achieve 10.46 % of efficiency with 70.50% of FF [35]. The simulated homo structure comprised of InN and Si substrate, which have a band gap of 0.65 eV and 1.124 eV, respectively. The basic parameter used in this solar cell with a 10 cm^2 device area is depicted in Figure 1. The basic parameter such as Si substrate was configured to be 350 µm thick, whereas the InN layer was designed to be 1×10^{-3} µm, while the doping concentrations of n- and p- regions are 1×10^{21} and 1×10^{17} cm^{-3}, respectively. For the study on the influence of thicknesses, 5 variation thicknesses were used at n-InN (0.001, 0.1, 0.2, 0.3 and 0.4 µm) and p-Si (0.2, 0.25, 0.3, 0.35, and 0.4 nm). For the study on the influence of various doping concentrations, the n-InN doping concentration was observed over five orders of magnitude $1x10^{17}$, $1x10^{18}$, $1x10^{19}$, $1x10^{20}$ and $1x10^{21}$ cm^{-3}, where the p-Si was observed throughout five orders of magnitude from $1x10^{14}$ to $1x10^{18}$ cm^{-3}. In this study, calculations for the influence of thickness and doping concentration were all carried out under ideal circumstances using the Air Mass 1.5 Global solar spectrum at a temperature of 25 °C and an incoming power density of 0.1 W/cm^2. Table 1 provides a summary of the specific data for the suggested parameter used on InN/p-Si-based solar cells.

In Figure 2, the values entered for the basic parameters utilized to simulate an InN/p-Si-based solar cell are shown. By optimizing the thickness and the doping concentration of the emitter layer in accordance with the data in Table 1, a 19.08% efficiency is attained. In order to produce more efficiency, this research aims to improve the performance of InN/p-Si-based solar cells. InN solar cells are distinguished by the influence of parameters like the thickness of n- and p-layers, doping concentration and temperature dependence.

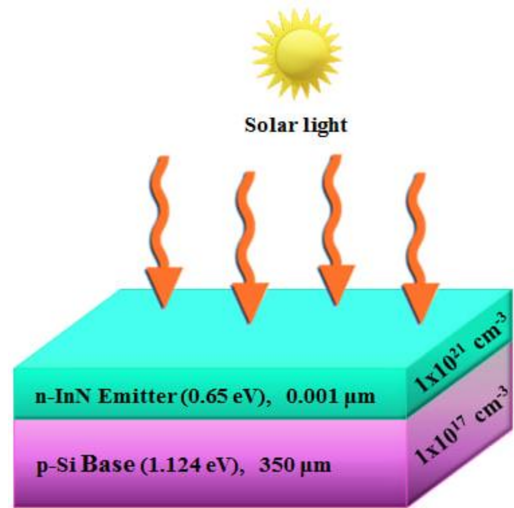

Figure 1: The schematic diagram of InN/p-Si-based solar cell

Table 1: Structure of the simulated InN/p-Si-based solar cell.

Parameter	Value	
Device area	10 cm^2	
Region	n-InN layer	p-Si layer
Thickness	0.001µm	350µm
Band gap	0.65 eV	1.124 eV
Intrinsic conc. (300K)	$2.25\times10^{13}cm^{-3}$	$1\times10^{10}cm^{-3}$
Background doping	$1\times10^{21}cm^{-3}$	$1\times10^{17}cm^{-3}$
Bulk recombination lifetime	2×10^{-3} µs	1000 µs
Dielectric constant	15.3	11.9
Refractive index	2.9	1.124
Excitation mode	One-sun (transient; 16 timesteps)	
Spectrum	AM1.5G	
Intensity	0.1W/cm^2	
Temperature	25°C	

DEVICE
Device area: 10 cm^2
No surface texturing
No surface charge
No Exterior Front Reflectance
No Exterior Rear Reflectance
No internal optical reflectance
Emitter contact enabled
Base contact enabled
No internal shunt elements
REGION 1
Thickness: 1×10^{-3} µm
Material modified from gan.mat
Fixed electron mobility: 400 cm^2/Vs
Fixed hole mobility: 10 cm^2/Vs
Dielectric constant: 15.3
Band gap: 0.65 eV
Intrinsic conc. at 300 K: 2.52×10^{13} cm^{-3}
Refractive index: 2.9
Absorption coeff. from inn.abs
Free carrier absorption enabled
N-type background doping: 1×10^{21} cm^{-3}
No front diffusion
No rear diffusion
Bulk recombination: $\tau_n = \tau_p = 2\times10^{-3}$ µs
No Front-surface recombination
No Rear-surface recombination

Device Schematic
E
B

REGION 2
Thickness: 350 µm
Material from si.mat
Carrier mobilities from internal model
Dielectric constant: 11.9
Band gap: 1.124 eV
Intrinsic conc. at 300 K: 1×10^{10} cm^{-3}
Refractive index from si.inr
Absorption coeff. from si300.abs
Free carrier absorption enabled
P-type background doping: 1×10^{17} cm^{-3}
No front diffusion
No rear diffusion
Bulk recombination: $\tau_n = \tau_p = 1000$ µs
No Front-surface recombination
No Rear-surface recombination
EXCITATION
Excitation from one-sun.exc
Excitation mode: Transient, 16 timesteps
Temperature: 25°C
Base circuit: Sweep from -0.8 to 0.8 V
Collector circuit: Zero
Primary light source enabled
Constant intensity: 0.1 W cm^{-2}
Spectrum from am15g.spc
Secondary light source disabled

Figure 2: Basic parameters used in PC1D simulation of InN/p-Si-based solar cell

The open circuit voltage, V_{oc} is provided by [1] as:

$$V_{oc} = \frac{kT}{q} \times ln\left(\frac{I_{sc}}{I_0} + 1\right) \quad (1)$$

where
q is the electron charge,
k is the Boltzmann's constant,
T is the temperature.
I_{sc} is the short circuit current,
I_o is the saturation current,

The maximum power is given by [2] as:

$$P_{max} = \eta\% \times P_{in} \quad (2)$$

where
P_{max} is the maximum power, and
P_{in} is the incident light power.

The incident light power is defined by [3] with the standard insolation denoted by [4] expression:

$$Pin = standard\ insolation \times area \quad (3)$$

$$Standard\ insolation = \frac{1kW}{m^2} \quad (4)$$

The cell conversion efficiency η of the cell is expressed as a percentage. It is defined [5] as:

$$\eta = \frac{P_{max}}{P_{in}} = \frac{V_{oc} \times I_{sc} \times FF}{P_{in}} \quad (5)$$

The fill factor (FF) is defined by [6]:

$$FF = \frac{I_m \times V_m}{I_{sc} \times V_{oc}} \quad (6)$$

where I_m and V_m are coordinates of the maximum power point.

In this study, the impacts of temperature on InN solar cells are also examined. The main result is that as the temperature rises, the band gap narrows. The electrical parameters of the suggested solar photovoltaic cell, particularly the J_{sc}, V_{oc}, and conversion efficiency (η), have been computed using an analytical solar cell model with the temperature dependency of the optical band gap and its effect.

J-V characteristic of the solar cell is given by [7]:

$$J = J_{sc} - J_0\left(e^{\frac{qV_{oc}}{kT}} - 1\right) \quad (7)$$

where
J_{sc} is the short circuit current density,
J_o is the saturation current density,

3. RESULTS AND DISCUSSION

The performance of InN/p-Si-based solar cells was examined by altering the thicknesses and the doping concentration for both the InN and Si layers. Figure 3 displays I-V characteristics of thicknesses of the InN layer starting from 0.001 to 0.04 µm. The characteristic shows how altering the InN layer thickness can change its efficiency. According to the graph, the highest curve corresponds to the thinnest layer of InN which is 0.001 µm. The highest current and output voltage occurs on the thinnest layer of InN while the lowest reading occurs on the thickest layer which is 0.04 µm. It is possible to increase the Jsc by reducing the front layer thickness [36] because it shortens the distance between the space charge region and the surface and therefore increases effective collecting efficiency [37]. Typically, as the thickness of the n-InN layer increases, the distance between the space charge area and the surface increases, increasing the potential of electron-hole recombination and decreasing the solar cell's I_{sc}.

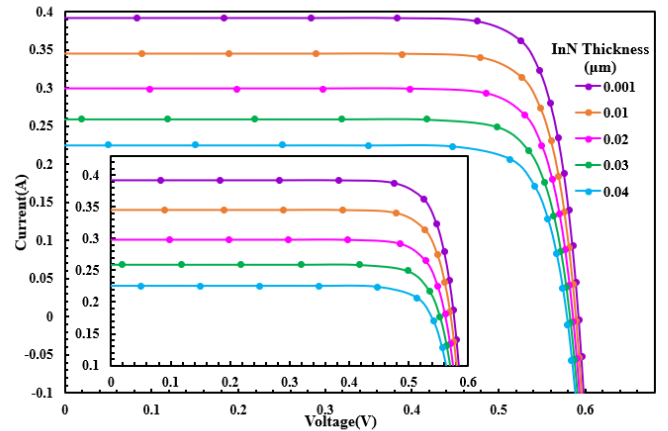

Figure 3: The effect of various thicknesses of n-InN

Table 2 indicates the reduced efficiency with the increase of InN thickness from 19.08% at 0.001 µm to 10.66% at 0.04 µm. This demonstrates that changes in InN thickness influenced all cell parameters, since the value attained at the short circuit was followed by an increase in the value of the open circuit voltage and fill factor, and thus an increase in the value of the conversion efficiency, since they are directly related to the rate of energy absorption. Due to the high absorption coefficient of III-Nitrides, very thin layers of material are required to absorb most incoming photons [38]. The optimal efficiency of the influence of thickness at InN was attained at the thinnest layer, which is 0.001 µm at 19.08% η with Voc = 0.5927 V, Isc = 0.3917 A, Pmax = 0.2411 W and FF = 82.18%.

Table 2: Output parameters on different thicknesses of InN

N-region Thickness, (µm)	I_{sc} (A)	V_{oc} (V)	P_{max} (W)	FF	η (%)
0.001	0.3917	0.5927	0.1908	0.8218	19.08
0.01	0.3446	0.5894	0.1664	0.8193	16.64
0.02	0.2990	0.5857	0.1445	0.8251	14.45
0.03	0.2594	0.5820	0.1246	0.8253	12.46
0.04	0.2251	0.5784	0.1066	0.8186	10.66

Figure 4 illustrates the effect of Si substrate thickness on the performance of the InN/p-Si solar cell. The I-V characteristics reveal that the thickness of the silicon substrate can have an effect on their efficiency. The maximum current value is obtained when the thickness of the Si substrate is 400 µm, the highest current value is obtained, and the lowest current value is obtained when the thickness is 200 µm. The impacts of increasing layer thickness at the p-region gradually enhanced efficiency. In comparison to the p-region curves of an InN/p-Si solar cell, the I-V characteristic indicates an increase in efficiency and voltage value as the thickness grows from 200 µm to 400 µm.

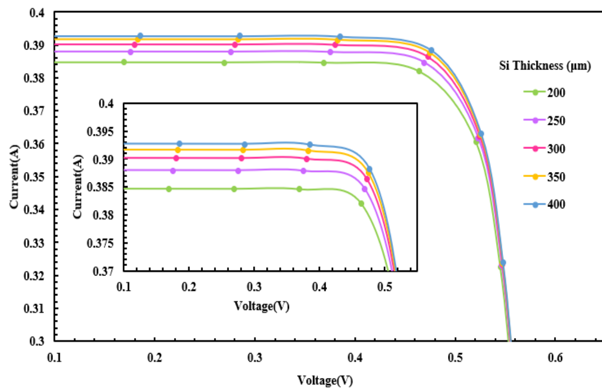

Figure 4: The I-V curve of influence of thickness at Si substrate

According to Table 3, the efficiency of p-region thickness increases as thickness increases. At the thickest layer of the Si substrate, the optimum efficiency of the InN solar cell was achieved, which is 400 µm at 19.13% efficiency with V_{oc} = 0.5927 V, I_{sc} =0.3927 A, P_{max} = 0.1913 W and FF = 0.8219. The circuit current gradually increases with the increment of the Silicon substrate thickness from 0.3847 A at 200 µm to 0.3927 A at 400 µm.

Table 3: Output parameters on different thicknesses at Si substrate

P-region Thickness (µm)	I_{sc} (A)	V_{oc}(V)	P_{max} (W)	FF	η (%)
200	0.3847	0.5922	0.1878	0.8243	18.78
250	0.388	0.5925	0.1892	0.8230	18.92
300	0.3902	0.5926	0.1902	0.8225	19.02
350	0.3917	0.5927	0.1908	0.8218	19.08
400	0.3927	0.5927	0.1913	0.821	19.13

The current research additionally investigates the influence of different doping concentrations on InN/p-Si-based solar cells. The amount of doping on the surface determines the level of light absorption and impacts the efficiency of solar cells [39]. The concentration of the material is also a key factor in estimating efficiency [40]. Figure 5 displays the effect of doping concentration on the InN. The n-region doping concentration was observed over five orders of magnitude $1x10^{17}$, $1x10^{18}$, $1x10^{19}$, $1x10^{20}$ and $1x10^{21}$ cm^{-3}. The circuit current and the circuit voltage slightly increase with the increase of the doping concentration from $1x10^{17}$ to $1x10^{21}$ cm^{-3}.

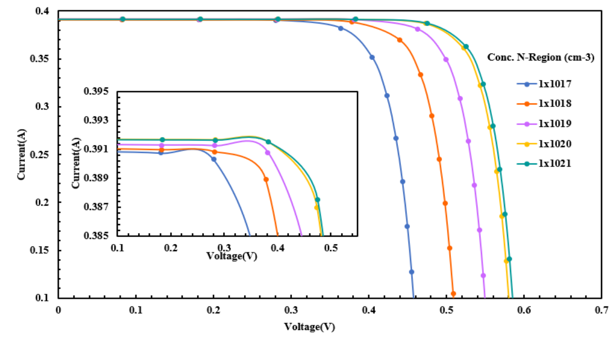

Figure 5: I-V characteristic for the influence of doping concentration at InN substrate

In general, surface recombination plays an important role in any solar cell's conversion efficiency. However, minority charge carriers limit the surface recombination velocity. Typically, minority charge carriers can be minimized by increasing the doping level in an n-type material p-n junction solar cell. Numerous studies have revealed that the optical properties of InN are significantly dependent on the deposition technique and intrinsic doping concentration [41]. The performance for the influence of doping concentration at InN demonstrates that efficiency increases as doping concentration increases. Based on Table 4, the I_{sc} increases when the doping concentration increases from 0.3909 A at $1x10^{17}$ cm^{-3} until 0.3913 A at $1x10^{19}$ cm^{-3} and the current remains the same with 0.3917 A at $1x10^{20}$ cm^{-3} and $1x10^{21}$ cm^{-3}. The efficiency increases when the doping concentration increases and reaches the lowest percentage of 14.27 % at a doping concentration of $1x10^{17}$ cm^{-3}. However, the doping concentration of n-region InN/p-Si solar cell optimized at $1x10^{21}$ cm^{-3} with efficiency of 19.08%, V_{oc} = 0.7417 V, I_{sc} =0.3887 A, P_{max} = 0.2411 W and FF = 0.8362. To optimize the performance of a solar cell, the precise amount of minority carrier concentration is required since surface recombination velocity is dependent on the minority carrier, which can reduce a solar cell's conversion efficiency.

Table 4: Output parameters on different doping concentrations at InN substrate

N-region doping concentration, (cm^{-3})	I_{sc} (A)	V_{oc} (V)	P_{max} (W)	FF	η (%)
$1x10^{17}$	0.3909	0.4654	0.1427	0.7843	14.27
$1x10^{18}$	0.3911	0.5169	0.1633	0.8077	16.33
$1x10^{19}$	0.3913	0.5576	0.1791	0.8208	17.91
$1x10^{20}$	0.3917	0.5883	0.1891	0.8206	18.91
$1x10^{21}$	0.3917	0.5927	0.1908	0.8218	19.08

Figure 6 depicts the outcome of doping concentration on the Si substrate. The concentration of Si layer doping was measured throughout five orders of magnitude from $1x10^{14}$ to $1x10^{18}$ cm^{-3} respectively. The open circuit voltage increases from $1x10^{14}$ cm^{-3} to $1x10^{16}$ cm^{-3} and starts to decrease until $1x10^{18}$ cm^{-3}. The maximum current occurred at $1x10^{16}$ cm^{-3}, as indicated in Figure 6. Furthermore, increasing the p-region doping concentration would raise the rate closer to the interface, reducing efficiency [42]. A Si substrate with a doping concentration of $1x10^{18}$ cm^{-3} has the lowest short-circuit current. However, the current and voltage starts to drop when the doping concentration is

over 1x10^{16} cm^{-3}. The crystal structure was harmed by the excessive doping density, which reduced the performance of the solar cells by forming a shunt channel in the solar cell [43].

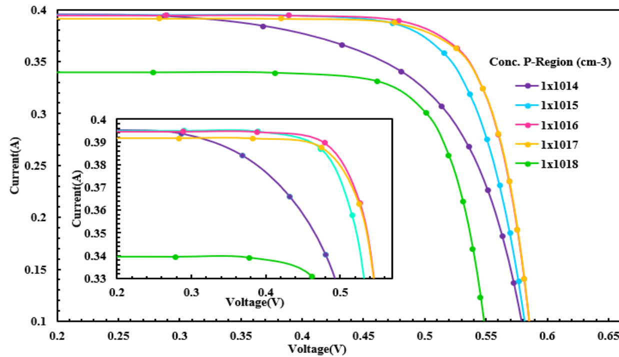

Figure 6: The influence of doping concentration of Silicon substrate.

Table 5 demonstrates that the circuit current declines from the lowest to the highest doping concentration. The lowest efficiency was attained on the doping concentration of 1x10^{16} cm^{-3} at 15.5 %. The optimal efficiency of the Si region doping concentration was achieved at 1x10^{16} cm^{-3} with 19.18 % with V_{oc} = 0.0.5933 V, I_{sc} = 0.3945 A, P_{max} = 0.1918 W and FF = 0.8195.

Table 5: Output parameters on different doping concentrations at Silicon substrate.

P-region doping concentration, (cm^{-3})	I_{sc} (A)	V_{oc} (V)	P_{max} (W)	FF	η (%)
$1x10^{14}$	0.3952	0.5925	0.1636	0.6986	16.36
$1x10^{15}$	0.3949	0.5926	0.186	0.7948	18.6
$1x10^{16}$	0.3945	0.5933	0.1918	0.8194	19.18
$1x10^{17}$	0.3917	0.5927	0.1908	0.8218	19.08
$1x10^{18}$	0.3394	0.5572	0.155	0.8196	15.5

Figure 7 shows the *P-V* and I-V characteristics, and Table 6 lists the combinations of the various parameters that generate the best efficiency. According to the graph below, InN/p-Si solar cells can achieve a greater efficiency of 19.18 % under these optimal circumstances.

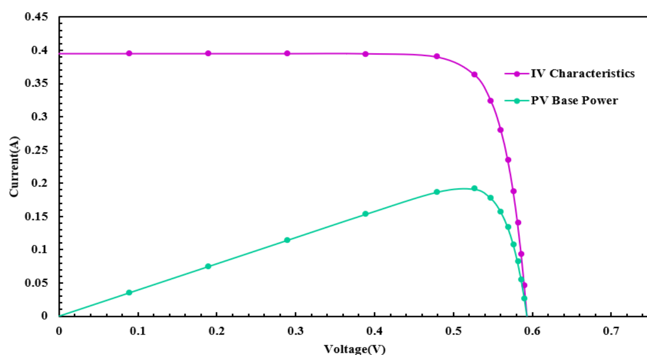

Figure 7: Graph of I-V and P-V curves

Table 6 illustrates the output parameters of the InN/p-Si solar cell with the highest efficiency. The ideal parameter values are attained at V_{oc} = 0.5933V, I_{sc} = 0.3945A, P_{max} = 0.1918W and FF = 0.8195. The fill factor and efficiency were computed using the algorithm, and the resulting efficiency percentage was 19.18 %. The single junction InN/p-Si solar cell's efficiency rises to 19.18% as a result of optimizing the thickness and doping concentration at both n-p regions using PC1D simulation. Figure 8 depicts the *J-V* characteristics of the InN/p-Si solar photovoltaic cell for various temperatures varying from 200K to 400K. As the optical bandgap shrinks, the short circuit current density (J_{sc}) marginally rises as temperature rises. Additionally, the solar cell reacts to the infrared component of the solar spectrum, and J_{sc} rises as temperature rises. The V_{oc} drops significantly from 0.79 V at 200 K to 0.38 V at 400 K. This can be attributed to the material band gap contracting as the temperature increases.

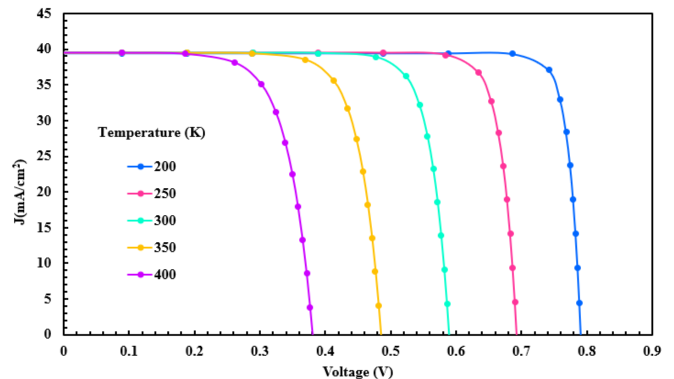

Figure 8: *J-V* characteristics of the InN/p-Si solar cell as a function of temperatures

Figure 9 depicts the behaviour of the conversion efficiency (η) as a function of temperature for the InN/p-Si-based solar cell. The J_{sc} and V_{oc} are essential variables to determine the solar cell's conversion efficiency. It is well known that when the temperature of the solar cell rises, the increase in J_{sc} is unable to make up for the decrease in V_{oc} [44]. The solar cell's conversion efficiency decreased as the temperature increased. This is also brought on by the band gap narrowing as the temperature rises [45]. The optical band gap energy decreases with increasing temperature, and this decrease is caused by an enormous rise in reverse saturation current density [46].

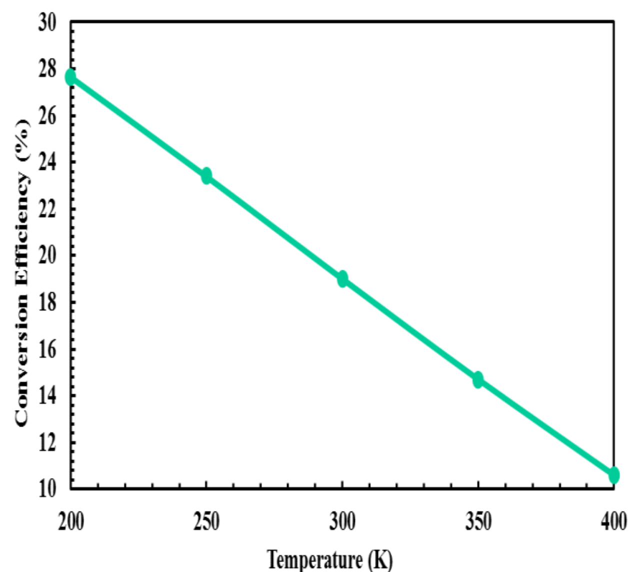

Figure 9: The conversion efficiency of the InN/p-Si solar cell versus temperatures

Table 7: Theoretically calculated basic electrical parameters of InN/p-Si solar cell

Temperature (K)	J_{sc} **(mA/cm²)**	V_{oc} **(V)**	**Efficiency,** η **(%)**
200	39.44	0.79	27.67
250	39.45	0.69	23.40
300	39.45	0.59	19.01
350	39.46	0.48	14.07
400	39.47	0.38	10.59

The efficiency of the InN/p-Si solar cell gradually decreased from 27.67 % to 10.59 % when the temperature was increased from 200 K to 400 K. The basic electrical parameters of the InN/p-Si solar cell under AM1.5G ($0.1 W/cm^2$) 200 K, 250 K, 300 K, 350 K and 400 K were summarized in Table 7. The optimal efficiency attained with temperature dependence on InN/p-Si solar cell was attained at 200 K which is the lowest temperature with 27.67 %, V_{oc} = 0.79 V and J_{sc} = 39.44 mA/cm^2. The InN/p-Si solar cell's performance is heavily influenced by the temperature because a reduction in temperature may greatly improve conversion efficiency.

4. CONCLUSIONS

In this study, PC1D was used to model single InN/p-Si-based p-n junction solar cells. We have demonstrated how to enhance the solar cell simulation's PC1D software's application of solar cell parameters. The results showed that solar cells with thickness (doping concentration) of n-InN and p-Si layers are 0.001 μm (10^{21} cm^{-3}) and 350 μm (10^{16} cm^{-3}), respectively, had the highest η of 19.18 %. The temperature has been proven to have an adverse effect on the efficiency of InN/p-Si-based solar cells, as was expected. Although the J_{sc} slightly increased with temperature, the loss in V_{oc} has a significant impact and causes the efficiency to decline as the temperature rose. We have demonstrated that the most effective values for n-reg thickness, p-reg thickness, n-reg doping concentration, p-reg doping concentration and temperature are 0.001 μm, 350 μm, 10^{21} cm^{-3}, 10^{16} cm^{-3} and 200 K, respectively, with η of 27.67 %.

ACKNOWLEDGMENTS

The financial support from Universiti Teknologi Mara, Shah Alam, Malaysia is gratefully acknowledged.

REFERENCES

[1] A. Khettou, I. Zeydi, M. Chellali, M.B. Arbia, S. Mansouri, H. Helal, and H. Maaref, “Simulation and optimization of InGaN Schottky solar cells to enhance the interface quality,” *Superlattices and Microstructures*, vol. 142, p. 106539, 2020.

[2] R. Kour, S. Arya, S. Verma, A. Singh, P. Mahajan, and A. Khosla, “Recent advances and challenges in indium gallium nitride (InGaN) materials for solid state lighting,” *ECS Journal of Solid State Science and Technology*, vol. 9, no. 1, p. 015011, 2019.

[3] M. Yamaguchi, F. Dimroth, J.F. Geisz, and N.J. Ekins-Daukes, “Multi-junction solar cells paving the way for super high-efficiency,” *Journal of Applied Physics*, vol. 129, no. 24, 2021.

[4] Y. Zhao, M. Xu, X. Huang, J. Lebeau, T. Li, D. Wang, and H. Jiang, “Toward high efficiency at high temperatures: Recent progress and prospects on InGaN-based solar cells,” *Materials Today Energy*, vol. 101229, 2022.

[5] C. Boudaoud, A. Hamdoune, and Z. Allam, “Simulation and optimization of a tandem solar cell based on InGaN,” *Mathematics and Computers in Simulation*, vol. 167, pp. 194-201, 2020.

[6] R. Belghouthi and M. Aillerie, “Temperature dependence of InGaN/GaN Multiple quantum well solar cells,” *Energy Procedia*, vol. 157, pp. 793-801, 2019.

[7] I. Segmene, Y. Sayad, N. Selatni, and A. Nouiri, “Design guidelines of InGaN nanowire arrays for photovoltaic applications,” *International Journal of Nano Dimension*, vol. 12, no. 4, pp. 393-401, 2021.

[8] A.E. Aouami, L.M. Pérez, K. Feddi, M. El-Yadri, F. Dujardin, M.J. Suazo, and E.M. Feddi, “Influence of Geometrical Shape on the Characteristics of the Multiple InN/In_xGa_{1−x}N Quantum Dot Solar Cells,” *Nanomaterials*, vol. 11, no. 5, p. 1317, 2021.

[9] C. Weisbuch, S. Nakamura, Y.R. Wu, and J.S. Speck, “Disorder effects in nitride semiconductors: impact on fundamental and device properties,” *Nanophotonics*, vol. 10, no. 1, pp. 3-21, 2020.

[10] A.N. Khan, K. Jena, G. Chatterjee, and S. Routray, “An Approach Towards Low Cost III-Nitride GaN/InGaN Solar Cell: the Use of Si/SiCN Substrate,” *Silicon*, 2022.

[11] E. Pelucchi, G. Fagas, I. Aharonovich, D. Englund, E. Figueroa, Q. Gong, and K.D. Jöns, “The potential and global outlook of integrated photonics for quantum technologies,” *Nature Reviews Physics*, vol. 4, no. 3, pp. 194-208, 2022.

[12] H. Shen, D. Walter, Y. Wu, K.C. Fong, D.A. Jacobs, T. Duong, and K.R. Catchpole, “Monolithic perovskite/Si tandem solar cells: pathways to over 30% efficiency,” *Advanced Energy Materials*, vol. 10, no. 13, p. 1902840, 2020.

[13] M.A. Green and S.P. Bremner, “Energy conversion approaches and materials for high-efficiency photovoltaics,” *Nature Materials*, vol. 16, no. 1, pp. 23-34, 2017.

[14] T.L. Tansley, E.M. Goldys, and M. Godlewski, “Electrical and Optical Properties of GaN,” *GaN and Related Materials*, vol. 233, 2021.

[15] Y. Sayad, “Photovoltaic potential of III-nitride based tandem solar cells,” *Journal of Science: Advanced Materials and Devices*, vol. 1, no. 3, pp. 379-381, 2016.

[16] S.S. Ng, H. San Lee, and Z.Y. Lee, “Sol–Gel Spin Coating Growth of Magnesium-Doped Indium Nitride Thin Films on Different Substrates,” *Engineering Journal*, vol. 24, no. 4, pp. 285-294, 2020.

[17] M. Azadmand, “PA-MBE Growth and Characterization of Nitride Semiconductors, from InGaN Thin-films to GaN and AlN Self-assembled Nanowires.”

[18] A.K. Tan, N.A. Hamzah, M.A. Ahmad, S.S. Ng, and Z. Hassan, “Parasitic behavior of different V/III ratios on the properties of InGaN/GaN heterostructures by MOCVD technique,” *Journal of Alloys and Compounds*, vol. 936, p. 168236, 2023.

[19] S.G. Kumar, A.P. Shetty, and C.R. Prashanth, "Solar cell material based on the optimum values of key parameters using PC1D," in *2021 2nd International Conference for Emerging Technology (INCET)*, pp. 1-6, IEEE, May 2021.
[20] A.B. Nawale, R.A. Kalal, A.R. Chavan, T.D. Dongale, and R.K. Kamat, "Numerical investigation of spatial effects on the silicon solar cell," *Журнал нано-та електронної фізики*, vol. 8, no. 2, p. 02002-1, 2016.
[21] G. Hashmi, A.R. Akand, M. Hoq, and H. Rahman, "Study of the enhancement of the efficiency of the monocrystalline silicon solar cell by optimizing effective parameters using PC1D simulation," *Silicon*, vol. 10, pp. 1653-1660, 2018.
[22] M. Subramanian, B. Nagarajan, A. Ravichandran, V. Subhash Betageri, G.S. Thirunavukkarasu, E. Jamei, and V.R. Minnam Reddy, "Optimization of Effective Doping Concentration of Emitter for Ideal c-Si Solar Cell Device with PC1D Simulation," *Crystals*, vol. 12, no. 2, p. 244, 2022.
[23] A. Bouadia, H. Naima, A. Djelloulc, Y. Benkrimad, and R. Farese, "Enhancing the efficiency of the gallium indium nitride (InGaN) solar cell by optimizing the effective parameters," *Chalcogenide Letters*, vol. 19, no. 9, pp. 611-619, 2022.
[24] S.H. Zyoud and A.H. Zyoud, "Simulation and Numerical Investigation of the Effect of Temperature and Defect on ZnTe/ZnSe/ZnO Thin-Film Photovoltaic Solar Cell Performance Efficiency."
[25] S. Valdueza-Felip, A. Núñez-Cascajero, R. Blasco, D. Montero, L. Grenet, M. De La Mata, and F. B. Naranjo, "Influence of the AlN interlayer thickness on the photovoltaic properties of in-rich AlInN on Si heterojunctions deposited by RF sputtering," *AIP Advances*, vol. 8, no. 11, 2018.
[26] Y. Cho, A. Yamaguchi, R. Uehara, S. Yasuhara, T. Hoshina, and M. Miyauchi, "Temperature dependence on bandgap of semiconductor photocatalysts," *The Journal of Chemical Physics*, vol. 152, no. 23, 2020.
[27] N.J. O'Brien, P. Rouf, R. Samii, K. Rönnby, S.C. Buttera, C.W. Hsu, and H. Pedersen, "In situ activation of an indium (III) triazenide precursor for epitaxial growth of indium nitride by atomic layer deposition," *Chemistry of Materials*, vol. 32, no. 11, pp. 4481-4489, 2020.
[28] A.K. Tan, N.A. Hamzah, M.A. Ahmad, S.S. Ng, and Z. Hassan, "Recent advances and challenges in the MOCVD growth of indium gallium nitride: A brief review," *Materials Science in Semiconductor Processing*, vol. 143, p. 106545, 2022.
[29] M. Sarollahi, M. Zamani-Alavijeh, R. Allaparthi, M.A. Aldawsari, M. Refaei, R. Alhelais, and M.E. Ware, "Study of simulations of double graded InGaN solar cell structures," *Journal of Vacuum Science & Technology B*, vol. 40, no. 4, 2022.
[30] T. Ataser, "The performance analysis of the GaAs/c-InN solar photovoltaic cell hetero-structure: temperature dependence," *Optical and Quantum Electronics*, vol. 52, no. 9, p. 407, 2020.
[31] B. Chouchen, M.H. Gazzah, A. Bajahzar, and H. Belmabrouk, "Numerical modeling of the electronic and electrical characteristics of InGaN/GaN-MQW solar cells," *Materials*, vol. 12, no. 8, p. 1241, 2019.
[32] S. Kissinger, "Indium Nitride Nanostructures Prepared by Various Growth Techniques," *J. Environ. Nanotechnol*, vol. 8, no. 4, pp. 38-44, 2019.
[33] Y. Zhao, M. Xu, X. Huang, J. Lebeau, T. Li, D. Wang, and H. Jiang, "Toward high efficiency at high temperatures: Recent progress and prospects on InGaN-based solar cells," *Materials Today Energy*, vol. 31, p. 101229, 2023.
[34] Z. Lin, M. Ragab, Z. Ren, J.W. Yoon, T. Buonassisi, V. Chellappan, and S. Jayavelu, "Transfer learning for material parameter extraction from current-voltage characteristics of solar cells."
[35] H.U. Manzoor, T. Kwan, N. Shiong, and Z. Hassan, "Carrier Density and Thickness Optimization of In," *Sains Malaysiana*, vol. 51, no. 5, pp. 1567-1576, 2022.
[36] F. Chen, X. Ji, and S.P. Lau, "Recent progress in group III-nitride nanostructures: From materials to applications," *Materials Science and Engineering: R: Reports*, vol. 142, p. 100578, 2020.
[37] M. Mamta, K.K. Maurya, and V.N. Singh, "Comparison of various thin-film-based absorber materials: a viable approach for next-generation solar cells," *Coatings*, vol. 12, no. 3, p. 405, 2022.
[38] J. Wu and T. Wen, "Simulation Result of InGaN for Solar Cell Application," 2022.
[39] L.C. Andreani, A. Bozzola, P. Kowalczewski, M. Liscidini, and L. Redorici, "Silicon solar cells: toward the efficiency limits," *Advances in Physics: X*, vol. 4, no. 1, p. 1548305, 2019.
[40] D.K. Shah, K.C. Devendra, T.G. Kim, M.S. Akhtar, C.Y. Kim, and O.B. Yang, "Influence of minority charge carrier lifetime and concentration on crystalline silicon solar cells based on double antireflection coating: A simulation study," *Optical Materials*, vol. 121, p. 111500, 2021.
[41] Z. He, H. Huang, J. Huang, G. Xiang, J. Zhang, Z. Yue, and H. Wang, "Study on the effect of sputtering pressure on the physical properties of InN films on ITO substrate and the dependence of carrier transport characteristics of Li-doped p-NiO/n-InN heterojunction on the environmental temperature," *Vacuum*, vol. 220, p. 112833, 2024.
[42] D. Parajuli, D.K. Shah, D. KC, S. Kumar, M. Park, and B. Pant, "Influence of Doping Concentration and Thickness of Regions on the Performance of InGaN Single Junction-Based Solar Cells: A Simulation Approach," *Electrochem*, vol. 3, no. 3, pp. 407-415, 2022.
[43] F.H. Alharbi and S. Kais, "Theoretical limits of photovoltaics efficiency and possible improvements by intuitive approaches learned from photosynthesis and quantum coherence," *Renewable and Sustainable Energy Reviews*, vol. 43, pp. 1073-1089, 2015.
[44] M. Pospischil, T. Riebe, A. Jimenez, M. Kuchler, S. Tepner, T. Geipel, and F. Clement, "Applications of parallel dispensing in IV metallization," in *AIP Conference Proceedings*, vol. 2156, no. 1, 2019.
[45] M. Sarollahi, M. Zamani Alavijeh, M.A. Aldawsari, R. Allaparthi, R. Alhelais, M.A. Refaei, and M.E. Ware, "M. Sarollahi, M. Zamani Alavijeh, M.A. Aldawsari, R. Allaparthi, R. Alhelais, M.A. Refaei, and M.E. Ware, "Modeling of Λ-graded In x Ga1− x N solar cells: comparison of strained and relaxed features," Journal

of Photonics for Energy, vol. 12, no. 2, p. 022205, 2022.," *Journal of Photonics for Energy*, vol. 12, no. 2, p. 022205, 2022.

[46] M. O. Moustafa and T. Alzoubi, "Numerical simulation of single junction InGaN solar cell by SCAPS," *Key Engineering Materials*, vol. 821, pp. 407-413, 2019